

Length-Weight Relationship and Sagittal Otolith Morphometrics of *Diplodus sargus* (Linnaeus, 1758) from the Southwestern Mediterranean Sea: Using Multiple Analytical Approaches

Mansouri Toufik^{1,2}, Guendouzi Yassine³, Djezzar Miliani², Stransky Christoph⁴, Brückner Hendrik⁴ and Rohlf Norbert⁴

¹Department of Biology, Sciences of Nature and Life Faculty, Abdelhamid Ibn Badis University, Mostaganem, 27000, PO Box 300, Algeria

²ERP (Eau, Roches & Plantes) Laboratory, Djilali Bounaama University of Khemis Miliana, Theniet El Had Road, Soufay 44225 Khemis Miliana, Algeria

³Laboratory for the Management and Valorization of Agricultural and Aquatic Ecosystems, University Center of Tipaza Morsli Abdallah, Ouade Merzouk 4200, Tipaza, Algeria

⁴Thünen Institute of Sea Fisheries, Bremerhaven, Germany

*Corresponding Author: t.mansouri@univ-dbkm.dz

ARTICLE INFO

Article History:

Received: July 10, 2025

Accepted: Sep. 15, 2025

Online: Oct. 12, 2025

Keywords:

Shape analysis,
Otolith contours,
Stock discrimination,
Algeria

ABSTRACT

This study investigated the length-weight relationship and morphometric characteristics of sagittal otoliths of *Diplodus sargus* (Linnaeus, 1758), including contour shape analysis, using multiple analytical approaches. These approaches aim to characterize the otoliths' outlines and to explore their potential as a tool for biological and ecological discrimination. A sample of 102 *D. sargus* individuals was collected from fisheries in three locations representing different coastal regions of Algeria: Mostaganem (western coast), Tipaza (central coast), and Jijel (eastern coast). A significant positive correlation ($R^2 = 0.67$; $P < 0.05$) between total length (TL) vs. total weight (TW) was revealed. Isometric growth between length and weight was recorded in *D. sargus* individuals ($P > 0.05$). Significant inter-station differences in TL and TW indicated spatial heterogeneity in population structure. A morphometric analysis based on weight and shape indices was applied to assess the structural variability of the otoliths. No significant differences were detected between the two sagittal otoliths in terms of weight and morphometric parameters ($P > 0.05$: Wilcoxon test and paired t-test). Furthermore, contour analysis of the right sagittal otolith using the wavelet method revealed significant shape variation, particularly in *D. sargus* sampled from Mostaganem. This variation may reflect the influence of environmental and/or genetic factors on otolith contour morphology in this region.

INTRODUCTION

Sparids, commonly known as seabreams, are a family of teleost fish within the order Perciformes, comprising approximately 166 species distributed across 39 genera (Parenti, 2019). These fish predominantly inhabit tropical and temperate waters, with occasional occurrences in colder and brackish environments. They are demersal species, typically found on the continental shelf and upper slope. While smaller species and juveniles tend to be gregarious, adults generally adopt a solitary lifestyle (Fischer *et al.*, 1987). Sparids hold

significant ecological and economic importance due to their species richness and worldwide high commercial value (**Basurco *et al.*, 2011**).

The genus *Diplodus* includes 23 species, among which the white seabream, *Diplodus sargus* (Linnaeus, 1758), is one of the most widely distributed. Its geographical range extends across the Mediterranean, the western Black Sea, and the eastern Atlantic, from Brittany to the Canary Islands, Madeira, and northwestern Africa (**Giacalone *et al.*, 2022**). This demersal species is commonly found in beds, primarily inhabiting rocky and mixed substrates at depths of less than 50 meters, where it seeks refuge in crevices and holes during nighttime or to evade predators during daytime activities (**Harmelin, 1987; Sala & Ballesteros, 1997; Figueiredo *et al.*, 2005**).

Otoliths are biomineralized structures composed primarily of calcium carbonate, located in cavities on either side beneath the brain. The largest of these cavities houses the largest otolith, known as the sagitta, which plays a crucial role in hearing and balance (**Simonian, 2023**). Although otolith morphology varies significantly among species, it generally features a convex proximal inner surface and a concave distal outer surface. Typically, otolith growth is more pronounced along the anteroposterior axis compared to the dorsoventral axis. The external morphology of otoliths serves as a key diagnostic feature for species identification, making them valuable tools in archaeological studies and in research on predator-prey interactions within trophic networks (**Lowry, 2011; Disspain *et al.*, 2016; Stock *et al.*, 2021; Agiadi, 2022; Quigley *et al.*, 2023**). At the interspecific level, no direct correlation has been established between fish size and otolith size (**Campana, 2005a**). Consequently, pelagic species such as tuna and swordfish may possess relatively small otoliths, whereas certain small reef species exhibit disproportionately large otoliths (**Campana, 2005a**). Additionally, fish adapted for rapid swimming tend to have more elongated otoliths compared to benthic-demersal species (**Volpedo *et al.*, 2008; Tuset *et al.*, 2015**). Moreover, otolith contour analysis is a powerful tool for fisheries stock discrimination. Among the most widely used approaches, Fourier and wavelet methods allow precise characterization of otolith morphological variability and enable the identification of population differences based on geographic origin and environmental conditions (**Tracey *et al.*, 2006; Stransky, 2014**).

The objective of this study was to analyze the length-weight relationship of *D. sargus*, examine the morphometric parameters of its sagittal otoliths, and evaluate their relevance as tools for stock discrimination.

MATERIALS AND METHODS

1. Sampling

A total of 102 *D. sargus* individuals were collected from fisheries along three distinct regions of the Algerian coast: Jijel (eastern coast, n=12), Tipaza (central coast, n=60), and Mostaganem (western coast, n=30) (Fig. 1). The sampled individuals measured between 16 and 22 cm in total length and weighed from 50 to 577g.

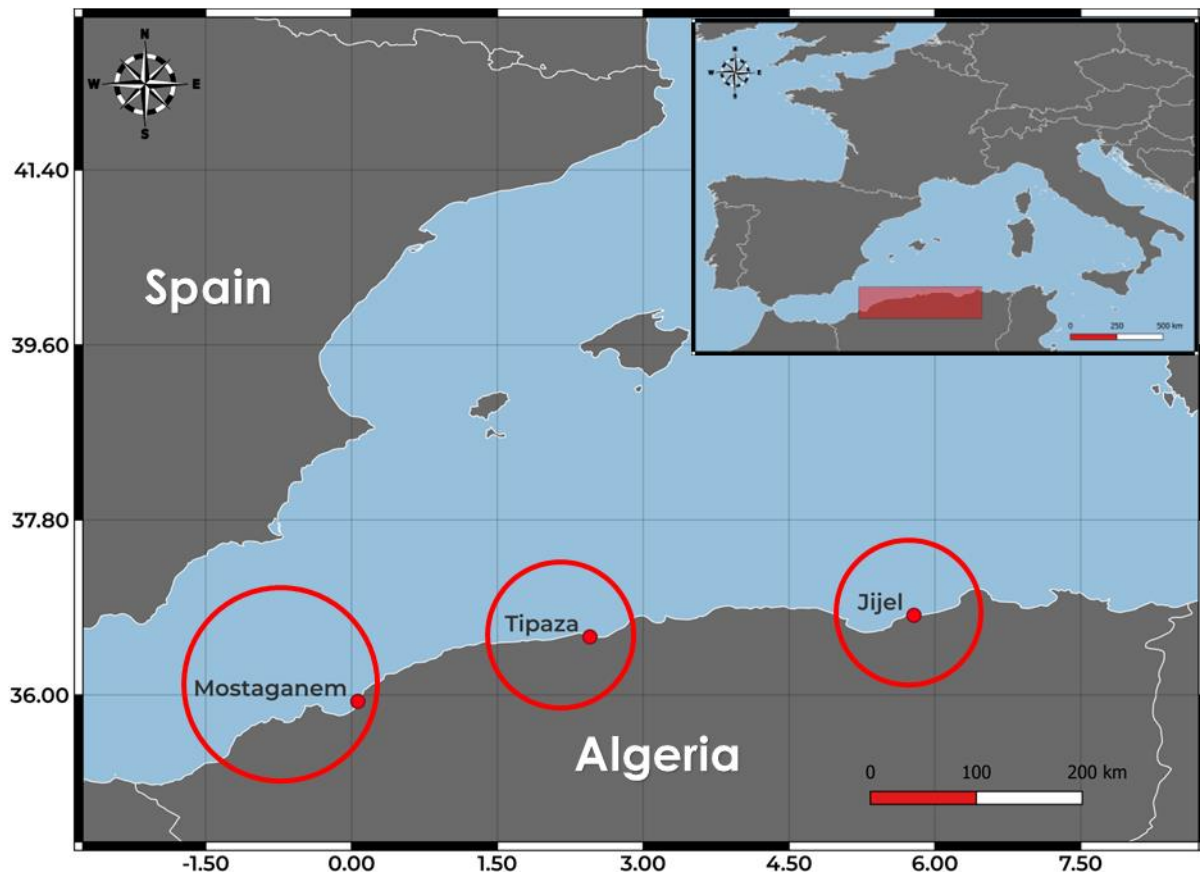


Fig. 1. Sampling stations of *D. sargus* individuals

The specimens were immediately placed in a cooler and transported to the laboratory of Management and Valorisation of Agricultural and Aquatic Ecosystems (GVEAA) at the university centre of Tipaza, Algeria. In the laboratory, the specimens were rinsed and photographed with a scale using a Canon Ixus 155 camera. The total body weight (TW) was then measured using a precision balance (0.1 mg accuracy).

The sagittal otoliths were carefully extracted from each individual, thoroughly cleaned, and preserved in labelled vials (Eppendorf, ®), which were stored in a dry environment (102 pairs of otoliths) (Fig. 2). Subsequently, the otoliths were transferred to the Thünen Institute of Sea Fisheries in Bremerhaven, Germany, for shape analysis. Intact sagittal otoliths were photographed using a high-resolution Leica M125-C digital stereomicroscope, with the *sulcus acusticus* facing upward and the rostrum oriented to the left in the horizontal plane to minimize

errors during normalization and digitization. Each otolith pair was then weighed using a SECURA225D-1S high-precision balance (SARTORIUS, accuracy: 10^{-5} g).

Finally, the total length (TL) of the individuals, along with the otolith morphometric parameters, was measured using the ImageJ software (version 1.54d).

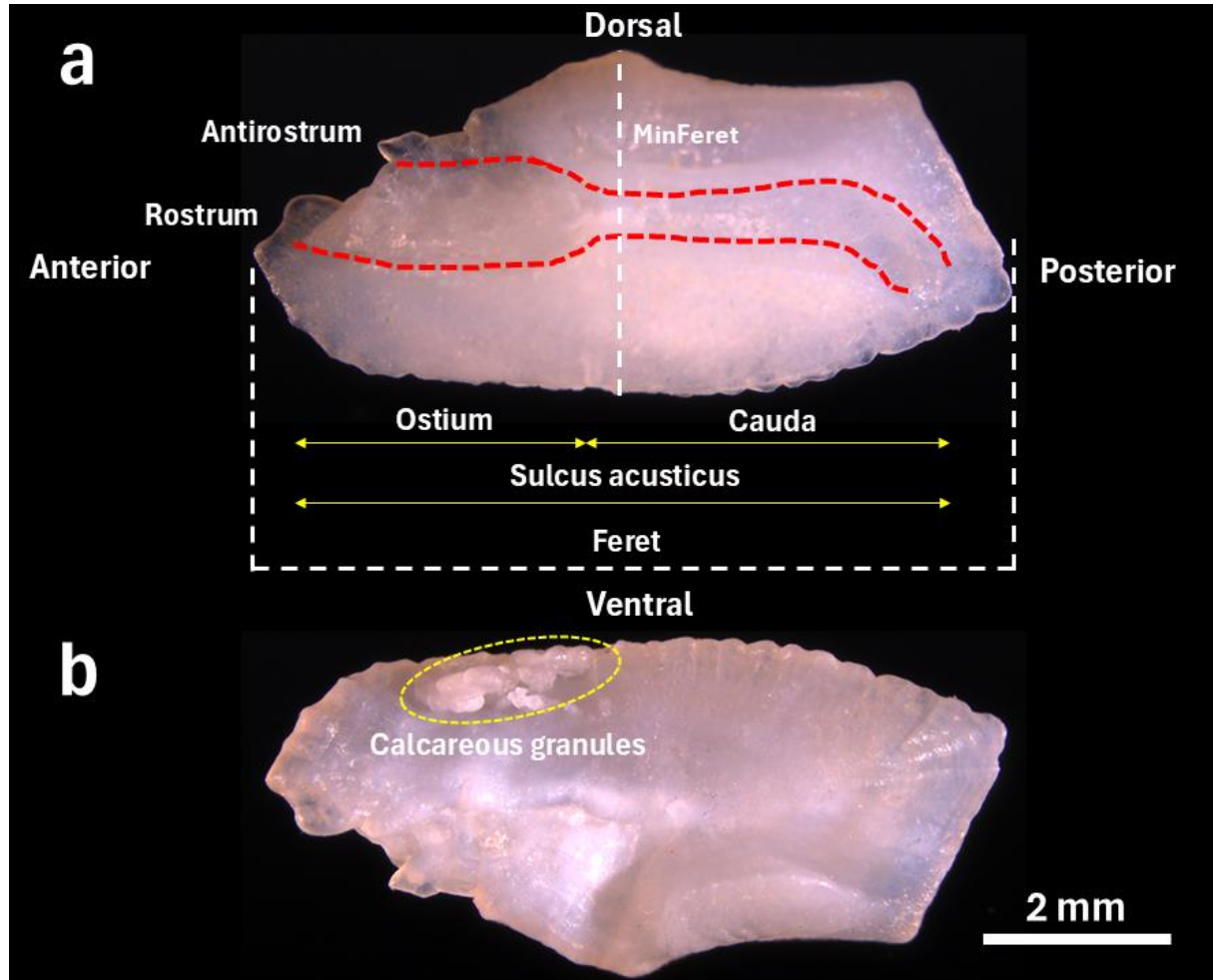


Fig. 2. Right sagittal otolith of *D. sargus*. (a) Proximal face and (b) Distal face

2. Biometry of *Diplodus sargus* and otolith morphometry

The length-weight relationships of *D. sargus* individuals were established, regardless of sex, using the formula $TW = a TL^b$ (Keys, 1928), where a is a constant and b is the regression slope or allometric coefficient. The constants a and b were estimated from the log-transformed values of length and weight using linear regression, represented by the equation $\log(TW) = b \log(TL) + \log(a)$. The length-weight relationship was used to establish the nature of growth (isometric or allometric) of the studied *D. sargus* individuals (Ricker, 1973). The significance of the regression was assessed using the F-statistic. To determine the nature of growth, the observed slope value (b) was compared to the theoretical value $b = 3$ (Sokal & Rohlf, 1995; Handjar *et al.*, 2022). When $b = 3$, growth is isometric; when $b < 3$, growth is hypoallometric; and if $b > 3$, growth is hyperallometric. In the case of isometry, body proportions grow at the same rate. However, in the latter two cases, the growth of a given parameter is proportionally lower or higher than that of the reference trait. Similarly, the significance of the deviation of the

slope b from the reference value ($b = 3$) was tested using Student's t -test via the FSA and FSAdat packages (Ogle *et al.*, 2025). Moreover, differences in *D. sargus*, total length (TL) and total weight (TW) among stations were tested using one-way ANOVA, following verification of residual normality (Shapiro–Wilk test) and variance homogeneity (Levene's test). If ANOVA assumptions were violated, the Kruskal–Walli's rank-sum test was employed (Zar, 2010).

Subsequently, the wavelet coefficients for each right sagittal otolith were calculated using the shape R package, following the protocol described by Libungan and Pálsson (2015). In addition, morphometric parameters, including area [ARE], perimeter [PRM], Feret diameter [FRD], minimum Feret diameter [MFRD], and a variety of shape indices (Table 1) were calculated for otoliths from both sides using the ImageJ software (Tuset *et al.*, 2003; Ponton, 2006).

Table 1. Morphometric variables and indices measured for each sagittal otolith

Index	Formula	Description
Circularity (CIR)	$4\pi \times (Area) / (Perimeter)^2$	Proximity to a perfect circle (1 = circle, <1 = less circular).
Ellipticity (ELP)	$(Feret - Minferet) / (Feret + Minferet)$	A value of 0 indicates symmetry; higher values reflect elongation along a primary axis.
Rectangularity (REC)	$(Area) / (Feret \times MinFeret)$	Similarity to a rectangle (1 = rectangle, <1 = irregular).
Aspect ratio (AR)	$(Feret) / (Minferet)$	Width-to-height ratio (1 = square-like, >1 = elongated).
Roundness (RND)	$4 \times (Area) / \pi \times (Feret)^2$	Smoothness and curvature (1 = round, <1 = irregular/angular).
Solidity (SLD)	$(Area) / (Convex\ area)$	Area vs. convex hull (1 = solid/convex, <1 = concave/fragmented).

3. Statistical analysis of otolith morphometrics

The significance of differences between left and right otoliths in terms of mean morphometric measurements was assessed using a paired t -test. However, before performing this test, the data were transformed using the Yeo-Johnson method. The normality of the otolith geometric data was evaluated using the Shapiro-Wilk test, while homoscedasticity of variances was checked using Fisher's F -test. Since the normality of otolith weights was not confirmed (Shapiro-Wilk test at $P < 0.05$), the non-parametric Wilcoxon signed-rank test was used instead of the paired t -test. In addition, a canonical analysis of principal coordinates [CAP] (Anderson

& Willis, 2003) was conducted to assess the variation in the contour shape of the right sagittal otolith from each individual among the three *D. sargus* populations. The CAP analysis was employed to explore the relationships between otolith shape and wavelet transformation coefficients. These coefficients capture variations in otolith contours and are used to analyze differences among populations. Subsequently, a permutation ANOVA ($n = 1000$ permutations) was performed to test the significance of the observed differences (Oksanen *et al.*, 2022). All statistical analyses were conducted using the R software, version 4.3.0.

RESULTS

1. Biometric analysis of *D. sargus* individuals

Average total length of *D. sargus* increases as follows: 18.15 ± 1.80 cm (Mostaganem), 18.50 ± 1.63 cm (Tipaza) and 20.46 ± 1.83 cm (Jijel), with a mean value of 18.63 ± 1.82 cm. The average body weight increases as follows: 120.14 ± 29.14 g (Tipaza), 139 ± 91.57 g (Mostaganem) and 179.92 ± 53.67 g (Jijel), with a mean value of 132.72 ± 59.9 g. The biometric analysis revealed a high correlation ($R^2 = 0.67$) between total body weight (TW) and total length (TL) with a statistically significant tendency ($P < 0.05$). The allometric coefficient value b is near to the isometric coefficient value, *i.e.*, $b = 3$ ($P > 0.05$) (Fig. 3). The analysis of total length (TL) revealed significant differences among stations (ANOVA, $F(2,99) = 8.24$, $P < 0.05$). In contrast, the distribution of total weight (TW) deviated significantly from normality (Shapiro–Wilk test, $P < 0.001$). Accordingly, a non-parametric Kruskal–Wallis test was employed, which indicated significant differences among stations ($\chi^2 = 14.24$, $df = 2$, $P < 0.05$).

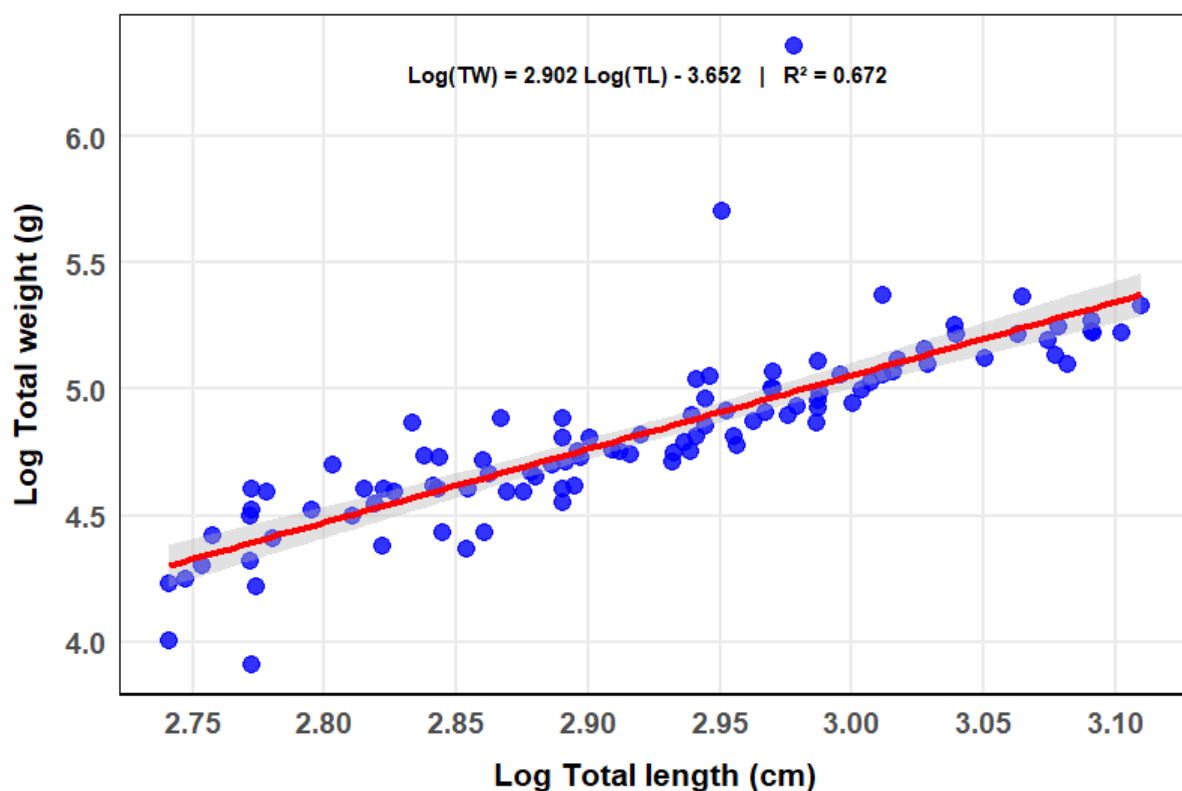


Fig. 3. Length–weight relationship of *D. sargus* from three stations of the Algerian coast

2. Otolith shape and morphometrics

The otolith shape of *D. sargus* revealed a heterosulcoid morphology (Fig. 2a), characterized by a *sulcus acusticus* with a clearly differentiated ostium and cauda. The ostium is funnel-shaped, and its length is equal to or shorter than that of the cauda. The cauda is tubular, curved, and distinctly bent posteriorly, terminating near the posteroventral edge (Fig. 2a). The distal face of the otolith is marked by the presence of calcareous granules arranged in clusters (Fig. 2b).

According to the weight and morphometric parameters, there is no statistically significant difference between the left and right sagittal otoliths ($P > 0.05$; Wilcoxon test and paired t-test; Table (2); Fig. (4)).

Table 2. Morphometric parameters and shape indices of the left and right sagittal otoliths of *Diplodus sargus*, collected from the Algerian coast

Morphometric parameters	*Left sagittal otolith	*Right sagittal otolith
Feret (mm)	6.45 ± 0.70 (4.63 – 9.88)	6.46 ± 0.63 (4.63 – 8.86)
MinFeret (mm)	3.25 ± 0.30 (2.65 – 4.70)	3.27 ± 0.29 (2.50 – 4.62)
Area (mm ²)	15.35 ± 3.06 (9.03 – 33.91)	15.45 ± 2.79 (8.61 – 30.63)
Perimeter (mm)	17.37 ± 1.84 (12.67 – 26.72)	17.46 ± 1.67 (12.55 – 25.30)
Weight (g)	0.02 ± 0.01 (0.01 – 0.06)	0.02 ± 0.01 (0.01 – 0.06)
Otolith shape indices	Left sagittal otolith	Right sagittal otolith
Circularity	0.64 ± 0.04 (0.34 – 0.71)	0.63 ± 0.04 (0.41 – 0.71)
Rectangularity	0.73 ± 0.02 (0.69 – 0.77)	0.73 ± 0.02 (0.69 – 0.77)
Ellipticity	0.33 ± 0.03 (0.26 – 0.39)	0.33 ± 0.03 (0.26 – 0.39)
Aspect ratios	2.06 ± 0.13 (1.76 – 2.35)	2.05 ± 0.13 (1.76 – 2.35)
Roundness	0.49 ± 0.03 (0.43 – 0.57)	0.49 ± 0.03 (0.42 – 0.57)
Solidity	0.96 ± 0.01 (0.93 – 0.98)	0.96 ± 0.01 (0.93 – 0.98)

*Results are expressed as mean ± s.d., (Min value – Max value). For each parameter, the statistically significant differences (paired t-test and Wilcoxon) are not significant ($P > 0.05$) among left and right sagittal otolith.

The left otolith of *D. sargus* exhibits a generally elliptical and moderately elongated shape, as revealed by the morphometric parameters. The Feret Diameter (FRD_L) range

between 4.63 and 9.88mm, while the minimum Feret diameter (MFRD_L) ranges from 2.65 to 4.70mm, pointing to a structure that is clearly longer than it is wide. The area (ARE_L) varies between 9.03 and 33.91mm², and the perimeter (PRM_L) ranges from 12.67 to 26.72mm, indicating some variation in otoliths size among individuals (Table 2 & Fig. 4). The elongated form is further reflected in the aspect ratio (AR_L), which ranges from 1.76 to 2.35, suggesting that the otolith's length is approximately twice its width. Shape descriptors such as circularity (CRL_L: 0.34–0.71) and roundness (RND_L: 0.43–0.57) confirm that the otolith deviates from a circular outline, instead tending toward a more oval or elliptical shape. The ellipticity values (ELP_L), ranging from 0.26 to 0.39, further reinforce this observation by quantitatively describing the elongation (Table 2 & Fig. 4). The contour of the left otolith appears to be smooth and regular, as indicated by the high solidity values (SLD_L: 0.93–0.98), meaning the edge is continuous with few irregularities. Likewise, the rectangularity values (REC_L: 0.69–0.77) suggest that the otolith fits well within a rectangular frame, without prominent projections or notches (Table 2 & Fig. 4).

In summary, the left otolith of *D. sargus* can be described as elongated, elliptical, and structurally compact, with a smooth outline and consistent form. Given that paired *t*-test revealed no significant differences between left and right sagittal otoliths, this description is likely representative of both sides.

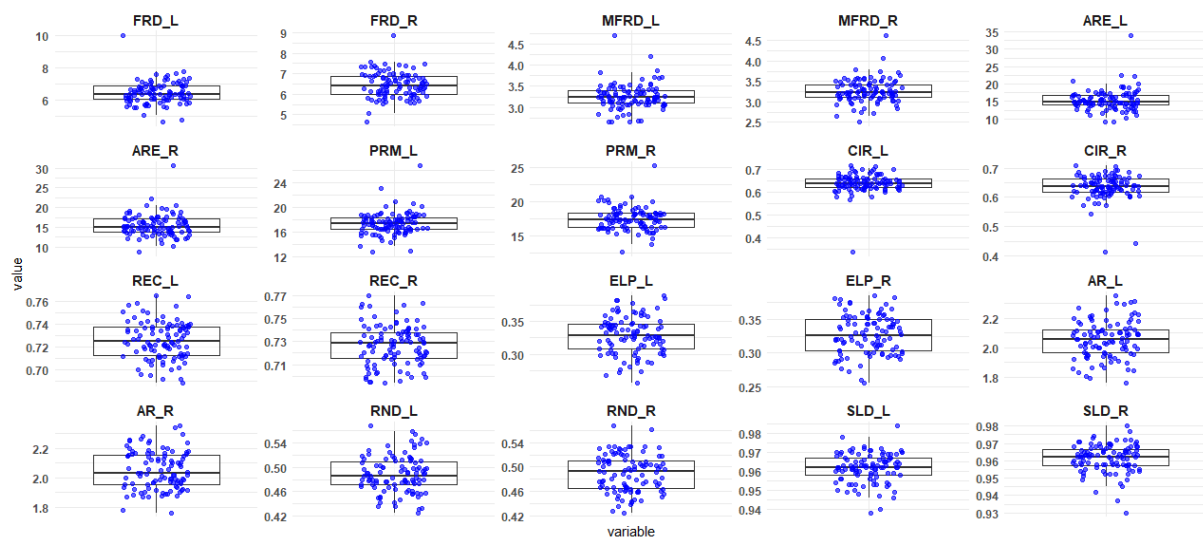


Fig. 4. Box plot of the morphometric measurements of the two sagittal otoliths of *D. sargus*, (R= right and L = left)

3. Otolith contour analysis

The analysis of the right sagittal otolith contours in *D. sargus* individuals revealed significant morphological differences among the three studied populations, particularly around the rostrum in the 160–210° and 340–359° ranges (Figs. 5 and 6). Moreover, within the 340–359° range, a marked deviation in the mean otolith contour of *D. sargus* from the Mostaganem station was observed compared with those from the other stations (Figs. 5, 6).

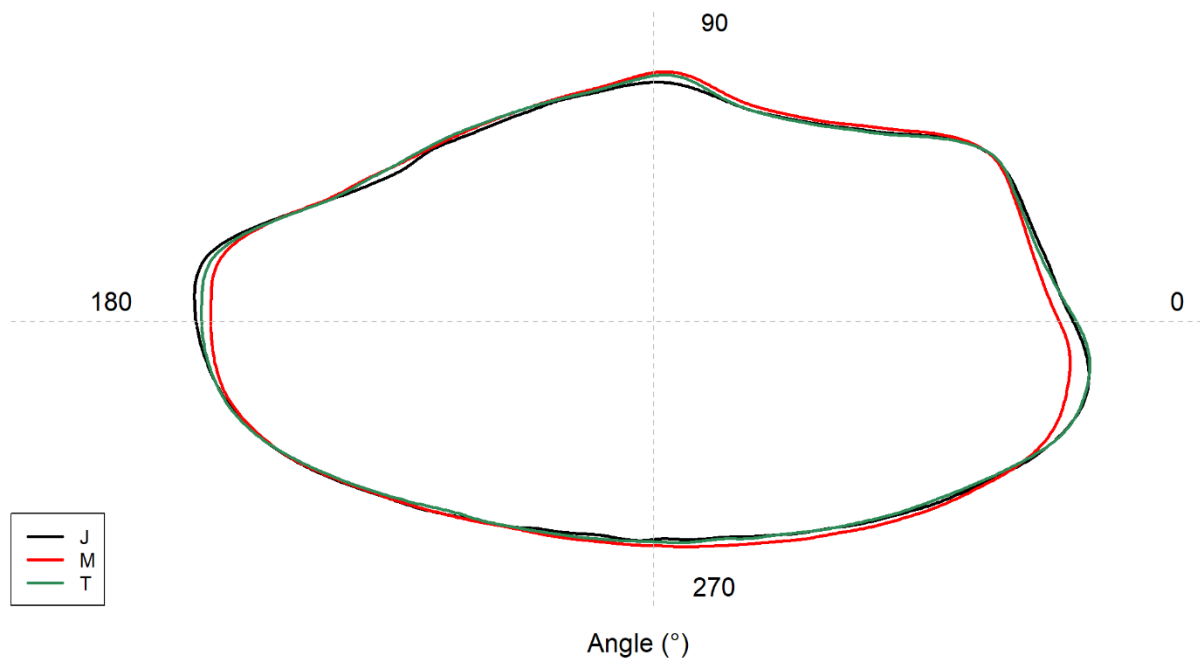


Fig. 5. Mean shape of the right sagittal otolith based on wavelet reconstruction for three discrete fish populations of *D. sargus* from the Algerian coast (J: Jijel, M: Mostaganem and T: Tipaza)

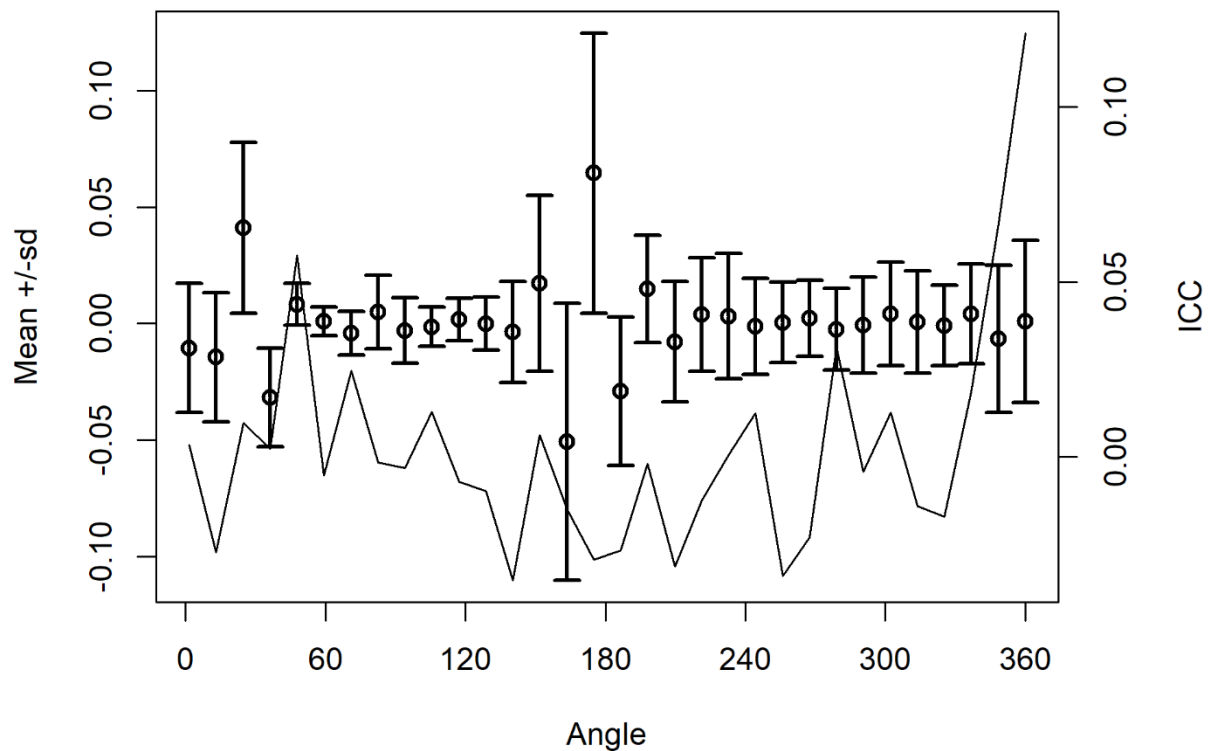


Fig. 6. Mean and standard deviation (s.d.) of wavelet coefficients for all combined right sagittal otoliths, with intraclass correlation (ICC, black solid line)

This morphological divergence is supported by the results of the canonical analysis of principal coordinates [CAP] (Fig. 7). Indeed, the CAP1 axis accounts for 87.71% of the variance, representing the primary factor differentiating the populations, while the CAP2 axis explains 12.29%, indicating additional but less variability. The distribution of individuals on the CAP plot reveals a broader dispersion of red points (Mostaganem), indicating higher morphological heterogeneity in this population. In contrast, the black (Jijel) and green (Tipaza) points exhibit noticeable overlap, suggesting a greater similarity in otolith shape between these two populations.

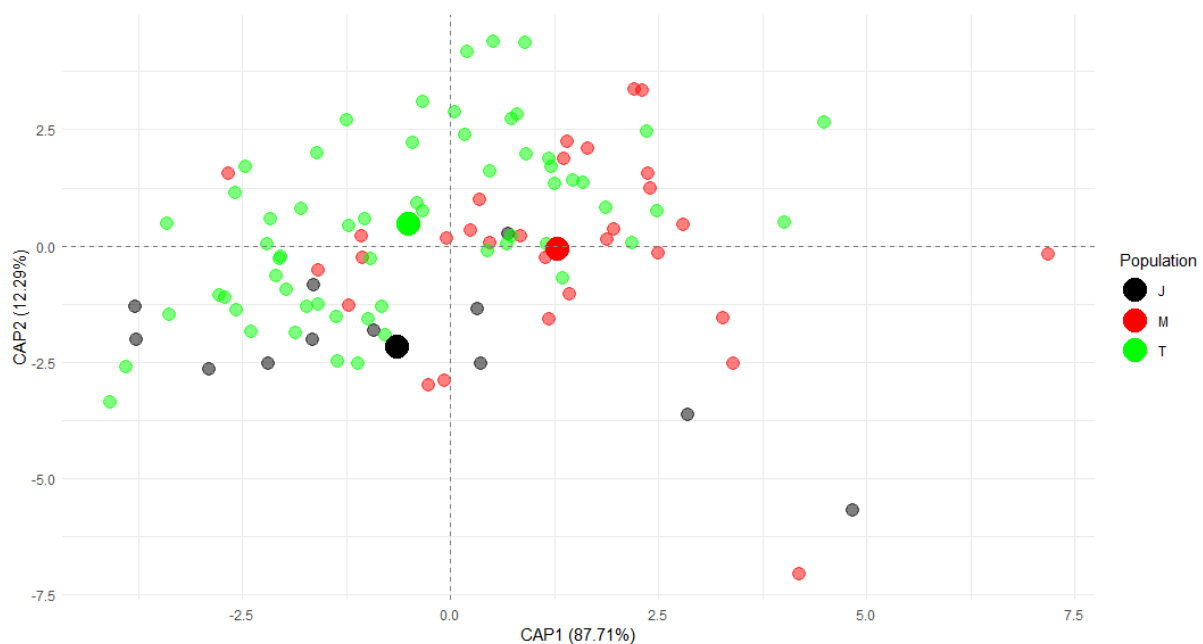


Fig. 7. Otolith shape of three *D. sargus* populations from the Algerian coast using canonical analysis of principal coordinates with the wavelet coefficients. (J: Jijel, M: Mostaganem and T: Tipaza). Big filled circles are barycentre's

The ANOVA like permutation test confirmed that this differentiation is statistically significant (CAP: $F(2, 99) = 3.22$, $P < 0.01$), highlighting the variability in otolith contours among populations, particularly between Mostaganem and the other two stations.

DISCUSSION

The growth of *D. sargus* across all studied areas was found to be isometric, indicating that (TW) increases at the same rate as (TL). According to **Lagler (1966)** and **Wootton (1990)**, isometric growth implies that fish maintain geometric similarity during ontogeny, with body proportions and specific gravity remaining essentially constant throughout their lifetime. This result was nearly similar to those obtained by **Man-Wai and Quignard (1982)** in the Gulf of Lion, France, **Morato *et al.* (2001)**, in the Azores, Portugal, **Mouine *et al.* (2007)**, in the Gulf

of Tunis, Tunisia, and by **Benchalel and Kara (2013)** as well as **Boufekane *et al.* (2021)** on the eastern and central Algerian coast (Algeria), respectively. The significant variation in length and weight among stations indicates spatial heterogeneity in *D. sargus* populations along the Algerian coast, potentially pointing to distinct population units. Such patterns are commonly reported in Mediterranean sparids (**Khedher *et al.*, 2021; Geladakis *et al.*, 2023**). Beyond somatic growth patterns, the analysis of otolith morphology provides additional insights into the biology of *D. sargus*. The heterosulcoid shape and the morphological features of *D. sargus* otoliths observed in this study are consistent with those described by **Tuset *et al.* (2008)** in the western Mediterranean. In addition, the presence of calcareous granules on the distal face agrees with the observations of **Shtewi *et al.* (2023)**. Therefore, the similarity of the shape and morphometric parameters between the left and right sagittal otoliths may be explained by the bilateral symmetry development of the otolith, which is regulated by genetic and physiological mechanisms (**Campana, 2005b**), and by the homogeneous environmental conditions e.g., temperature, salinity, and nutrition, which promote similar otolith growth (**Vignon & Morat, 2010**). Additionally, the absence of auditory dominance in fish leads to morphological symmetry between the left and right otoliths, thereby reducing morpho-geometric variability between them (**Lombarte & Cruz, 2007**). Furthermore, mechanical and behavioural constraints, particularly a balanced and symmetrical swimming mode, limit the occurrence of significant asymmetries in otolith structure (**Morat *et al.*, 2012**). This bilateral concordance in otolith shape and morphometrics is consistent with the findings of **Bostanci *et al.* (2016)** for another sparid e.g., *Diplodus puntazzo* (Walbaum, 1792) sampled from the Aegean Sea (Turkey), except for the ellipticity index, where a significant difference was observed. **Bourehail *et al.* (2015)** reported non-significant differences between the two *Sphyræna sphyræna* (Linnaeus, 1758) and sagittal otoliths of *Sphyræna viridensis* (Cuvier, 1829) collected from the Gulf of Annaba (Algeria, south-western Mediterranean), except for the circularity index. On the other hand, the variation in otolith contour shape, identified through wavelet analysis and particularly evident in *D. sargus* from the coast of Mostaganem, may be attributed to the proximity of Mostaganem to the Almería-Oran Front (AOF), a genetic barrier that restricts gene flow and promotes the emergence of morphological differences. According to **Bargelloni *et al.* (2005)**, the AOF represents a major barrier to the dispersal of marine populations in the Mediterranean and significantly influences their genetic structuring. These authors demonstrated that this barrier leads to genetic separation among marine populations, which could explain the observed variation in otoliths. Furthermore, a recent study on *Mytilus galloprovincialis* (Lamarck, 1819) revealed the presence of a mosaic hybrid zone extending 600 km along the Algerian coast, suggesting that this genetic barrier does not act as an absolute divide but rather as a gradual transition (**El Ayari *et al.*, 2019**). These results support the hypothesis that *D. sargus* populations on the Mostaganem coast undergo progressive differentiation influenced by the Almeria-Oran barrier. It has also been demonstrated that demersal species are more likely to be influenced by geographical barriers and hydrological fronts, restricting their movements and increasing the morphological differentiation of otoliths between stocks (**Mahé, 2019**). The mouth of Oued Cheliff, Algeria's largest Oued, is a major conduit for sediments and agricultural pollutants to the Mostaganem coast (**Belhadj *et al.*, 2006; Vandenbussche, 2017; Benkaddour, 2018**). This influx of contaminants, particularly

trace metals and pesticides, has led **Benkaddour (2018)** to identify a station at the Oued's mouth as a hotspot of anthropogenic inputs. The site exhibited extremely high conductivity (up to $80.0 \pm 0.1 \text{ mS}\cdot\text{cm}^{-1}$ during the wet season, far above the Algerian standard of $2.8 \text{ mS}\cdot\text{cm}^{-1}$), elevated dissolved salts and pollutants, an excessive organic load ($\text{COD/BOD}_5 = 7680$), and consistently high levels of suspended matter and sulphates. Water temperature ranged from 12.3 to 28.8°C , with pH values between 6.7 and 8.3 . Trace metal analyses revealed substantial concentrations of several trace metallic elements, including zinc (Zn , $13.3 \pm 1.6 \mu\text{g}\cdot\text{L}^{-1}$), manganese (Mn , $20.5 \pm 1.5 \mu\text{g}\cdot\text{L}^{-1}$), aluminium (Al , $92.3 \pm 1.7 \mu\text{g}\cdot\text{L}^{-1}$), arsenic (As , $2.24 \pm 0.01 \mu\text{g}\cdot\text{L}^{-1}$), and lead (Pb , $0.5 \pm 0.1 \mu\text{g}\cdot\text{L}^{-1}$). These extreme physicochemical conditions, indicative of chronic pollution, are likely to induce sublethal stress in *D. sargus* by disrupting metabolic pathways and otolith biomineralization, potentially contributing to the otolith contour shape deviations observed along the Mostaganem coast. Similar effects have been documented in *Dicentrarchus labrax* (Linnaeus, 1758) exposed to high pollutant concentrations (**Vandenbussche, 2017**), highlighting the broader ecological consequences of Oued inflow and coastal contamination on fish growth and development. It has also been shown that depth also influences otolith morphology (**Tuset *et al.*, 2003**). It is therefore likely that the individuals of this sparid sampled at Mostaganem evolved in habitats located at different isobaths from those at the Tipaza and Jijel stations, which could explain the morphological differences observed. These bathymetric variations could lead to morpho-functional adaptations of the otoliths in response to the specific constraints of their environment.

CONCLUSION

This study provided a general overview of the length-weight relationship in the sparid *D. sargus* sampled in three areas along the Algerian coast. We recorded isometric growth and a good correlation between the measured parameters (TL & TW). Our results of allometric relationships corroborate those of previous studies carried out on the same species. The observed differences in length and weight of *D. sargus* along the Algerian coast mirror those documented in other Mediterranean sparids. In addition, the general examination of *D. sargus* sagittal otoliths morphology revealed a heterosulcoid shape characterized by an elongated, elliptical form, structural compactness, and a smooth, consistent outline. Similarly, morphometric analysis of the sagittal otoliths of *D. sargus* revealed no significant differences between pairs of otoliths from the same individual. This uniformity seems to result from the bilateral symmetry of otolith development, homogeneous environmental conditions and the absence of auditory dominance, which act together to limit the morphological asymmetries of the otoliths. Analysis of the contours of *D. sargus* otoliths revealed a marked differentiation between the Mostaganem population and those of Tipaza and Jijel. This morphological variation could be attributed to the influence of the Almeria-Oran (AOF) genetic barrier, which limits gene flow and favours the emergence of differences between the studied sparids. However, the presence of a hybrid mosaic zone along the Algerian coast suggests that this barrier acts progressively rather than absolutely. Furthermore, the differentiation observed could also be the result of local environmental factors, in particular the influence of the Oued Cheliff, the main vector of sediments and agricultural contaminants toward the Mostaganem coast. The accumulation of pollutants, such as heavy metals and pesticides, is likely to alter

otolith development by generating physiological stress in juvenile of *D. sargus*. These disturbances could modify calcium depositions and, consequently, otolith morphology. Additionally, depth variations in the habitat could also play a role in shaping otolith structure. Changes in hydrostatic pressure, temperature, and nutrient availability at different depths may influence otolith growth patterns and mineralization processes, further contributing to the morphological differentiation observed between populations, underlining the importance of taking these elements into account when studying the structuring of populations of this sparid on the Algerian coast.

ETHICAL STATEMENT

This study involved the collection of otoliths from *D. sargus* individuals that were already dead at the time of sampling. No live animals were used, handled, or subjected to any experimental procedures. Therefore, in accordance with Algerian animal welfare regulations, ethical approval from the Algerian Committee on Ethics in Animal Experimentation was not required.

ACKNOWLEDGMENTS

The first author would like to express his sincere gratitude to Mr. Aimen MANSOURI and the local fishermen for their invaluable contributions to this study. Their support and collaboration were essential to the completion of this work. He would also like to extend his appreciation to the Thünen Institute of Sea Fisheries for their warm welcome and the assistance provided by its staff. In particular, he thanks Hendrik BRÜCKNER for his help in capturing the otolith photographs.

DECLARATIONS OF INTERESTS

The authors declare that they have no conflicts of interest relevant to the content of this article.

FUNDING INFORMATION

No funding was received from public, commercial, or not-for-profit organizations for the conduct of this study.

REFERENCES

- Agiadi, K. (2022).** The Fossil Otolith Record of Fishes (Vertebrata: Teleostei) in Greece. In: *Fossil Vertebrates of Greece Vol. 1: Basal vertebrates, Amphibians, Reptiles, Afrotherians, Glires, and Primates*; Vlachos, E., Ed.; Springer International Publishing, pp. 143–183.
- Anderson, M.J. and Willis, T.J. (2003).** Canonical analysis of principal coordinates: a useful method of constrained ordination for ecology. *Ecology*, 84(2), 511–525. [https://doi.org/10.1890/0012-9658\(2003\)084\[0511:CAOPCA\]2.0.CO;2](https://doi.org/10.1890/0012-9658(2003)084[0511:CAOPCA]2.0.CO;2)
- Bargelloni, L.; Alarcon, J.A.; Alvarez, M.C.; Penzo, E.; Magoulas, A.; Palma, J. and Patarnello, T. (2005).** The Atlantic–Mediterranean transition: Discordant genetic

- patterns in two seabream species, *Diplodus puntazzo* (Cetti) and *Diplodus sargus* (L.). *Molecular Phylogenetics and Evolution*, 36(3), 523–535. <https://doi.org/10.1016/j.ympev.2005.04.017>
- Basurco, B.; Lovatelli, A. and García, B. (2011).** Current Status of Sparidae Aquaculture. In: *Sparidae*; Pavlidis, M.A. and Mylonas, C.C., Eds.; Wiley-Blackwell, pp. 1–50.
- Belhadj, M.; Ghezzar, M.R.; Abdelmalek, F.; Benhamed, A.A.; Ouddane, B. and Addou, A. (2006).** Assessment of the Sediments Contamination by Heavy Metals of the Cheliff River, Algeria. *Journal of Environmental Science and Technology*, 3(3), 186–192.
- Benchalel, W. and Kara, M.H. (2013).** Age, growth and reproduction of the white seabream *Diplodus sargus sargus* (Linnaeus, 1758) off the eastern coast of Algeria. *Journal of Applied Ichthyology*, 29(1), 64–70. <https://doi.org/10.1111/j.1439-0426.2012.02057.x>
- Benkaddour, B. (2018).** *Contribution à l'étude de la contamination des eaux et des sédiments de l'Oued Chéliff (Algérie)* [Doctoral dissertation]. Université de Blida.
- Bostanci, D.; Yilmaz, M.; Yedier, S.; Kurucu, G.; Kontas, S.; Darçin, M. and Polat, N. (2016).** Sagittal Otolith Morphology of Sharpsnout Seabream *Diplodus puntazzo* (Walbaum, 1792) in the Aegean Sea. *International Journal of Morphology*, 34(2), 484–488. <https://doi.org/10.4067/S0717-95022016000200013>
- Boufekane, B.; Chakroun-Marzouk, N.; Kelai, E.; Alioua, Z.; Amira, S.; Harchouche, K. and Sciences, A. (2021).** Reproductive traits and somatic growth of *Diplodus sargus sargus* (Linnaeus, 1758) in the central Algerian coast (southern Mediterranean Sea). *Turkish Journal of Fisheries and Aquatic Sciences*, 21(8), 381–399. https://doi.org/10.4194/1303-2712-v21_8_01
- Bourehail, N.; Morat, F.; Lecomte-Finiger, R. and Kara, M.H. (2015).** Using otolith shape analysis to distinguish barracudas *Sphyræna sphyraena* and *Sphyræna viridensis* from the Algerian coast. *Cybium*, 39(4), 271–278.
- Campana, S.E. (2005a).** Otolith science entering the 21st century. *Marine and Freshwater Research*, 56(5), 485–495. <https://doi.org/10.1071/MF04170>
- Campana, S.E. (2005b).** Otolith Science: A Major Advance in Fish Ageing and Ecology. *Marine and Freshwater Research*, 56(5), 485–495. <https://doi.org/10.1071/MF04170>
- Disspain, M.C.F.; Ulm, S. and Gillanders, B.M. (2016).** Otoliths in archaeology: Methods, applications and future prospects. *Journal of Archaeological Science: Reports*, 6, 623–632. <https://doi.org/10.1016/j.jasrep.2015.05.012>
- El Ayari, T.; Trigui El Menif, N.; Hamer, B.; Cahill, A.E. and Bierne, N. (2019).** The hidden side of a major marine biogeographic boundary: a wide mosaic hybrid zone at the Atlantic-Mediterranean divide reveals the complex interaction between natural and genetic barriers in mussels. *Heredity*, 122(6), 770–784. <https://doi.org/10.1038/s41437-018-0174-y>
- Figueiredo, M.; Morato, T.; Barreiros, J.P.; Afonso, P. and Santos, R.S. (2005).** Feeding ecology of the white seabream, *Diplodus sargus*, and the ballan wrasse, *Labrus bergylta*, in the Azores. *Fisheries Research*, 75(1-3), 107–119. <https://doi.org/10.1016/j.fishres.2005.04.013>
- Fischer, W.; Bauchot, M.L. and Schneider, M. (1987).** *Fiches FAO d'identification des espèces pour les besoins de la pêche. (Rev 1). Méditerranée et mer Noire. Zone de Pêche 37. Vertébrés 2.* FAO.

- Geladakis, G.; Batargias, C.; Somarakis, S. and Koumoundouros, G. (2023).** Stock Discrimination of Gilthead Seabream (*Sparus aurata* Linnaeus, 1758) through the Examination of Otolith Morphology and Genetic Structure. *Fishes*, 8(6), 291. <https://doi.org/10.3390/fishes8060291>
- Giacalone, V.M.; Pipitone, C.; Abecasis, D.; Badalamenti, F. and D'Anna, G. (2022).** Movement ecology of the white seabream *Diplodus sargus* across its life cycle: a review. *Environmental Biology of Fishes*, 105(12), 1809–1823. <https://doi.org/10.1007/s10641-022-01258-0>
- Handjar, H.; Guendouzi, Y.; Niar, A.; Kara, H. and Benhalima, M. (2022).** Stock status of the bogue *Boops boops* (Walbaum, 1792) in Algerian West Coast (Southwestern Mediterranean Sea). *Regional Studies in Marine Science*, 56, 102727. <https://doi.org/10.1016/j.rsma.2022.102727>
- Harmelin, J.-G. (1987).** Structure and variability of the ichthyofauna in a Mediterranean protected rocky area (National Park of Port-Cros, France). *Marine Ecology*, 8(3), 263–284. <https://doi.org/10.1111/j.1439-0485.1987.tb00188.x>
- Keys, A.B. (1928).** The Weight-Length Relation in Fishes. *Proceedings of the National Academy of Sciences of the United States of America*, 14(12), 922–925.
- Khedher, M.; Mejri, M.; Shahin, A.A.B.; Quignard, J.P.; Trabelsi, M. and Ben Faleh, A.R. (2021).** Discrimination of *Diplodus vulgaris* (Actinopterygii, Sparidae) stock from two Tunisian lagoons using otolith shape analysis. *Journal of the Marine Biological Association of the United Kingdom*, 101(4), 743–751. <https://doi.org/10.1017/S0025315421000667>
- Lagler, K.F. (1966).** *Freshwater Fishery Biology*. W.C. Brown Co.
- Libungan, L.A. and Pálsson, S. (2015).** ShapeR: An R Package to Study Otolith Shape Variation among Fish Populations. *PLOS ONE*, 10(3), e0121102. <https://doi.org/10.1371/journal.pone.0121102>
- Lombarte, A. and Cruz, A. (2007).** Otolith size and shape: The importance of auditory sensitivity. *Journal of Morphology*, 268(2), 112–122. <https://doi.org/10.1002/jmor.10504>
- Lowry, M.S. (2011).** *Photographic Catalog of California Marine Fish Otoliths: Prey of California Sea Lions (Zalophus californianus)*. NOAA Technical Memorandum NMFS-SWFSC-481.
- Mahé, K. (2019).** *Variation of Otolith Shape: Implications of Stock Identification* [Habilitation Thesis]. Université du Littoral Côte d'Opale.
- Man-Wai, R. and Quignard, J. (1982).** Croissance linéaire et pondérale des jeunes *Diplodus sargus* 0+ (Pisces, Osteichthyes, Sparidae) des étangs Languedociens de Mauguio et du Prévost. *Revue des Travaux de l'Institut des Pêches Maritimes*, 45(4), 253–269.
- Morat, F.; Letourneur, Y. and Dierking, J. (2012).** The impact of locomotion and behavior on fish otolith shape: A multidisciplinary approach. *Journal of Experimental Marine Biology and Ecology*, 420–421, 55–64. <https://doi.org/10.1016/j.jembe.2012.03.003>
- Morato, T.; Afonso, P.; Lourinho, P.; Barreiros, J.P.; Santos, R.S. and Nash, R.D.M. (2001).** Length–weight relationships for 21 coastal fish species of the Azores, north-

- eastern Atlantic. *Fisheries Research*, 50(3), 297–302. [https://doi.org/10.1016/S0165-7836\(00\)00215-0](https://doi.org/10.1016/S0165-7836(00)00215-0)
- Mouine, N.; Francour, P.; Ktari, M.-H. and Chakroun-Marzouk, N. (2007).** The reproductive biology of *Diplodus sargus sargus* in the Gulf of Tunis (central Mediterranean). *Scientia Marina*, 71(3), 461–469. <https://doi.org/10.3989/scimar.2007.71n3461>
- Ogle, D.H.; Doll, J.C.; Wheeler, A.P. and Dinno, A. (2025).** *FSA: Simple Fisheries Stock Assessment Methods*. R package version 0.9.7.
- Oksanen, J.; Simpson, G.; Blanchet, F.; Kindt, R.; Legendre, P.; Minchin, P.; O'Hara, R.; Solymos, P.; Stevens, M.; Szoecs, E. and Wagner, H. (2022).** *Vegan: Community Ecology Package*. R package version 2.6-4.
- Parenti, P. (2019).** An annotated checklist of the fishes of the family Sparidae. *FishTaxa*, 4(1), 47–98.
- Ponton, D. (2006).** Is geometric morphometrics efficient for comparing otolith shape of different fish species? *Journal of Morphology*, 267(6), 750–757. <https://doi.org/10.1002/jmor.10439>
- Quigley, L.A.; Caiger, P.E.; Govindarajan, A.F.; McMonagle, H.; Jech, J.M.; Lavery, A.C.; Sosik, H.M. and Llopiz, J.K. (2023).** Otolith characterization and integrative species identification of adult mesopelagic fishes from the western North Atlantic Ocean. *Frontiers in Marine Science*, 10, 1146169. <https://doi.org/10.3389/fmars.2023.1146169>
- Ricker, W.E. (1973).** Linear regressions in fishery research. *Journal of the Fisheries Research Board of Canada*, 30(3), 409–434. <https://doi.org/10.1139/f73-072>
- Sala, E. and Ballesteros, E. (1997).** Partitioning of space and food resources by three fish of the genus *Diplodus* (Sparidae) in a Mediterranean rocky infralittoral ecosystem. *Marine Ecology Progress Series*, 152, 273–283. <https://doi.org/10.3354/meps152273>
- Shtewi, H.H.; Ensair, H.A.; Alhemmal, E.M. and Shuwaihi, S.Y. (2023).** Morphological characteristics of sagittae for *Diplodus sargus* and *D. vulgaris* (Perciformes: Sparidae) of Tripoli coast, Libya. *African Journal of Advanced Pure and Applied Sciences*, 2, 1–10.
- Simonian, M. (2023).** *Analyse de la diversité morphologique des otolithes chez les poissons Myctophiformes* [Doctoral dissertation]. Université de Montpellier.
- Sokal, R.R. and Rohlf, F.J. (1995).** *Biometry: The Principles and Practices of Statistics in Biological Research* (3rd ed.). W.H. Freeman.
- Stock, M.; Nguyen, B.; Courtens, W.; Verstraete, H.; Stienen, E. and De Baets, B. (2021).** Otolith identification using a deep hierarchical classification model. *Computers and Electronics in Agriculture*, 180, 105883. <https://doi.org/10.1016/j.compag.2020.105883>
- Stransky, C. (2014).** Morphometric Outlines. In: *Stock Identification Methods* (2nd ed.); Cadrin, S.X.; Kerr, L.A. and Mariani, S., Eds.; Academic Press, pp. 129–140.
- Tracey, S.R.; Lyle, J.M. and Duhamel, G. (2006).** Application of elliptical Fourier analysis of otolith form as a tool for stock identification. *Fisheries Research*, 77(2), 138–147. <https://doi.org/10.1016/j.fishres.2005.10.013>
- Tuset, V.; Lozano, I.; Gonzalez, J.; Pertusa, J. and Garcia-Diaz, M. (2003).** Shape indices to identify regional differences in otolith morphology of comber, *Serranus cabrilla* (L.,

- 1758). *Journal of Applied Ichthyology*, 19(2), 88–93. <https://doi.org/10.1046/j.1439-0426.2003.00344.x>
- Tuset, V.M.; Imondi, R.; Aguado, G.; Otero-Ferrer, J.L.; Santschi, L.; Lombarte, A. and Love, M. (2015). Otolith patterns of rockfishes from the northeastern pacific. *Journal of Morphology*, 276(4), 458–469. <https://doi.org/10.1002/jmor.20353>
- Tuset, V.M.; Lombarte, A. and Assis, C.A. (2008). Otolith atlas for the western Mediterranean, north and central eastern Atlantic. *Scientia Marina*, 72S1, 7–198. <https://doi.org/10.3989/scimar.2008.72s17>
- Vandenbussche, P. (2017). *Otolithes et bioindication : conséquence d'un stress environnemental sur la morphologie des sagittae de Dicentrarchus labrax et Oblada melanura* [Master's Thesis]. COMUE Université Côte d'Azur.
- Vignon, M. and Morat, F. (2010). Environmental and genetic determinant of otolith shape revealed by a non-inductive approach. *Marine Ecology Progress Series*, 411, 213–222. <https://doi.org/10.3354/meps08616>
- Volpedo, A.V.; Tombari, A.D. and Echeverría, D.D. (2008). Eco-morphological patterns of the sagitta of Antarctic fish. *Polar Biology*, 31(5), 635–640. <https://doi.org/10.1007/s00300-007-0400-1>
- Wootton, R.J. (1990). *Ecology of Teleost Fishes*. Chapman and Hall.
- Zar, J.H. (2010). *Biostatistical Analysis* (5th ed.). Prentice Hall/Pearson.

المخلص

تبحث هذه الدراسة في العلاقة بين الطول والوزن والخصائص المورفومترية للعظيومات السمعية السهمية (الأوتوليثات) لدى *Diplodus sargus* (Linnaeus, 1758)، بما في ذلك تحليل الشكل الخارجي للعظيومات باستخدام عدة مقاربات تحليلية. وتهدف هذه المقاربات إلى توصيف المحيط الخارجي للأوتوليثات واستكشاف إمكاناتها كأداة للتمييز البيولوجي والبيئي. تم جمع عينة مكونة من 102 فرداً من *D. sargus* من المصايد في ثلاث مناطق تمثل سواحل مختلفة من الجزائر: مستغانم (الساحل الغربي)، تيبازة (الساحل الأوسط)، وجيجل (الساحل الشرقي). وقد أظهرت النتائج وجود ارتباط إيجابي معنوي بين الطول الكلي (TL) والوزن الكلي (TW). كما تم تسجيل نمو متساوي القياس بين الطول والوزن لدى أفراد *D. sargus* ($P > 0.05$). بالإضافة إلى ذلك، برزت فروق معنوية في قيم الطول والوزن بين المحطات، ما يعكس تبايناً مكانياً في البنية السكانية وتم تطبيق تحليل مورفومتري يعتمد على الوزن ومؤشرات الشكل من أجل تقييم التباين البنيوي للأوتوليثات. ولم تُسجل فروق معنوية بين زوج الأوتوليثات السهمية من حيث الوزن أو العوامل المورفومترية (اختبار ويلكسون واختبار "ت" للعينات المرتبطة $P > 0.05$). علاوة على ذلك، كشف تحليل المحيط الخارجي للأوتوليث الأيمن باستخدام منهجية الموجات عن تباين معنوي في الشكل، خصوصاً لدى *D. sargus* المجمعة من مستغانم. وقد يعكس هذا التباين تأثير العوامل البيئية و/أو الوراثة على مورفولوجية محيط الأوتوليث في هذه المنطقة.

الكلمات المفتاحية: تحليل الشكل؛ محيط الأوتوليث؛ التمييز بين المخزونات؛ الجزائر.